Electronic Supplementary Information for:

End-capped group manipulation of fluorene-based small molecule acceptors for efficient organic solar cells

Jie Yang, Quan-Song Li*, and Ze-Sheng Li*

Beijing Key Laboratory of Cluster Science of Ministry of Education, Key Laboratory of Photoelectronic/Electrophotonic Conversion Materials, School of Chemistry and chemical engineering, Beijing Institute of Technology, Beijing 100081, China

E-mail: liquansong@bit.edu.cn, zeshengli@bit.edu.cn

Contents

Section S1 Calculation details on electron mobility

The Marcus theory[1, 2] with the hopping model was employed to describe the electron transport behavior. The charge hopping rate (*k*) is expressed as:[3, 4]

$$k = \frac{2\pi}{h} \mathrm{v}^2 \sqrt{4\pi\lambda k_B T} \exp\left[\frac{-(\Delta G + \lambda)^2}{4\lambda k_B T}\right]$$

where k_B represents the Boltzmann constant, T is the temperature in Kelvin, and *h* demotes the Planck constant. λ represents the reorganization energy, which is calculated using the adiabatic potential energy surface method. In this work, only internal reorganization energy which mainly originates from the geometrical relaxation during the charge transfer process and reflects the barriers from one molecule to another one, was considered. The reorganization energy can be expressed as follows:[5]

$$\lambda_{\mathrm{in}} = (E_0^* - E_0) + (E_-^* - E_-)$$

where E_0^* and E_-^* represent the total energies of neutral and anionic species with the geometries of anionic and neutral species, respectively. E_0 and E_- are the total energies of the neutral and anionic molecules in their lowest energy geometries, respectively.

v denotes the transfer integral, which is obtained by adopting a direct approach at the M06-2X/6-31G(d,p) level.[6] In our work, *v* can be written as:[7]

$$v = \left\langle \Psi_{\mathrm{i}}^{LUMO} | SC\varepsilon C^{-1} | \Psi_{\mathrm{f}}^{LUMO} \right\rangle$$

where $\psi_{\mathrm{i}}^{\mathrm{LUMO}}$ and $\psi_{\mathrm{f}}^{\mathrm{LUMO}}$ represent the LUMOs of the isolated molecules 1 and 2. The Kohn-Sham orbital *C* and eigenvalue ε were evaluated by diagonalizing the zeroth-order Fock matrix. *S* denotes the overlap matrix for the dimer. The electron mobility of the investigated molecules was calculated using the Einstein relation:[7, 8]

$$\mu = \frac{1}{2d} \frac{e}{k_B T} \sum r_{\mathrm{i}}^2 k_{\mathrm{i}} p_{\mathrm{i}}$$

where d represents the spatial dimensionality and is 3 in our work, i is a selected hopping pathway, r_{i} is the charge hopping centroid-to-centroid distance, and k_{i} denotes the charge hopping rate. P_{i} is defined as the hopping probability, which can be obtained using:

$$p_i = \frac{k_i}{\sum k_i}$$

Section S2 Details information on independent gradient model (IGM) analysis

Independent gradient model (IGM) method proposed by Corentin Lefebvre et al. can provide the descriptors of van der Waals interaction of some complexes, and its most attractive feature is that it can provide intermolecular or intramolecular interactions without selecting an isovalue. The interaction region in IGM can be represented by δg. The weak interactions in Multiwfn program can be calculated as follows:

$$\delta g = \left|\nabla \rho^{IGM}\right| - \left|\nabla \rho\right|$$

$$\delta g^{inter} = \left|\nabla \rho^{IGM,inter}\right| - \left|\nabla \rho\right|$$

where $\boldsymbol{\nabla \rho}^{\mathrm{IGM}}$ represents the total electron density gradient. $\delta g^{\mathrm{inter}}$ represents the δg function in the intermolecular regions which can describe the intermolecular interactions. All IGM analysis was performed by the Multiwfn 3.7 version.[9]

Section S3 Details about building the donor/acceptor interfaces

The studied donor/acceptor (D/A) interfaces of PBDB-TF/ITIC and PBDB-TF/A5_h were built in two steps. First, first principle molecular dynamics simulations were carried out with a D-A interval of 3.5 Å, referring to the reported configuration of PBDB-TF/ITIC.[10] The simulation temperature was set to 278 K, and the time step interval was 1 fs.[11] The NVE system and DFTB+1.2.1 software[12] were used. Next, the lowest energy configurations obtained by dynamic simulations were fully optimized at B3LYP-D3/6-31G(d) level with Gaussian 16 code.[13]

References

1. L. Tender, M. T. Carter and R. W. Murray, *Anal. Chem.*, 1994, **66**, 3173-3181.
2. J. M. Mayer, *Acc. Chem. Res.*, 2011, **44**, 36-46.
3. J. Cornil, J. L. Brédas, J. Zaumseil and H. Sirringhaus, *Adv. Mater.*, 2007, **19**, 1791-1799.
4. R. A. Marcus, *Rev. Mod. Phys.*, 1993, **65**, 599-610.
5. H.-Y. Chen and I. Chao, *Chem. Phys. Lett.*, 2005, **401**, 539-545.
6. Y. Zhao and D. G. Truhlar, *Theor. Chem. Acc.*, 2008, **120**, 215-241.
7. X. Yang, Q. Li and Z. Shuai, *Nanotechnology*, 2007, **18**, 424029.
8. V. Coropceanu, J. Cornil, D. A. da Silva Filho, Y. Olivier, R. Silbey and J.-L. Brédas, *Chem. Rev.*, 2007, **107**, 926-952.
9. T. Lu and F. Chen, *J. Comput. Chem.*, 2012, **33**, 580-592.
10. Q.-Q. Pan, S.-B. Li, Y.-C. Duan, Y. Wu, J. Zhang, Y. Geng, L. Zhao and Z.-M. Su, *Phys. Chem. Chem. Phys.*, 2017, **19**, 31227-31235.
11. I. Muhammad, H. Xie, U. Younis, Y. Qie, W. Aftab and Q. Sun, *Nanoscale*, 2019, **11**, 9000-9007.
12. B. Aradi and B. Hourahine, *DFTB+ Version 1.2, Density Functional Based Tight Binding, http://www.DFTB-Plus.Info*.
13. M. J. Frisch, G. W. Trucks, H. B. Schlegel, G. E. Scuseria, M. A. Robb, J. R. Cheeseman, G. Scalmani, V. Barone, G. A. Petersson, H. Nakatsuji, X. Li, M. Caricato, A. V. Marenich, J. Bloino, B. G. Janesko, R. Gomperts, B. Mennucci, H. P. Hratchian, J. V. Ortiz, A. F. Izmaylov, J. L. Sonnenberg, D. Williams-Young, F. Ding, F. Lipparini, F. Egidi, J. Goings, B. Peng, A. Petrone, T. Henderson, D. Ranasinghe, V. G. Zakrzewski, J. Gao, N. Rega, G. Zheng, W. Liang, M. Hada, M. Ehara, K. Toyota, R. Fukuda, J. Hasegawa, M. Ishida, T. Nakajima, Y. Honda, O. Kitao, H. Nakai, T. Vreven, K. Throssell, J. A. Montgomery, J. E. Peralta, F. Ogliaro, M. J. Bearpark, J. J. Heyd, E. N. Brothers, K. N. Kudin, V. N. Staroverov, T. A. Keith, R. Kobayashi, J. Normand, K. Raghavachari, A. P. Rendell, J. C. Burant, S. S. Iyengar, J. Tomasi, M. Cossi, J. M. Millam, M. Klene, C. Adamo, R. Cammi, J. W. Ochterski, R. L. Martin, K. Morokuma, O. Farkas, J. B. Foresman and D. J. Fox, *Gaussian 16, Revision A.03, Gaussian, Inc., Wallingford CT*, 2016, **3**.

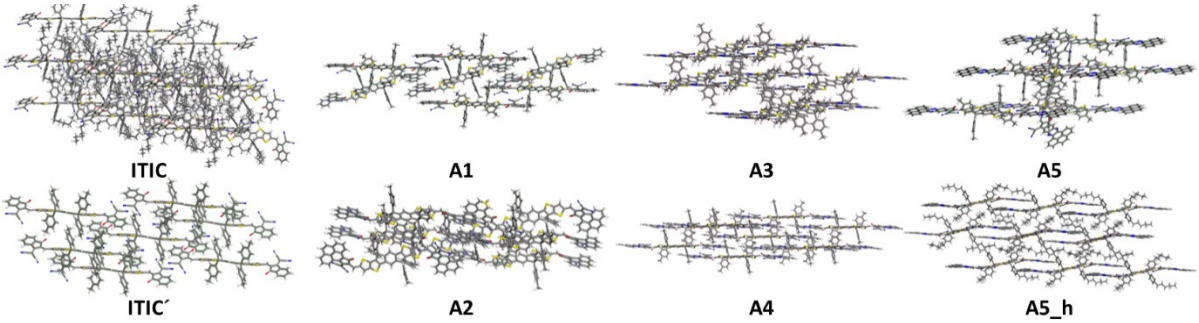

Fig. S1 The stacking structures for studied acceptors.

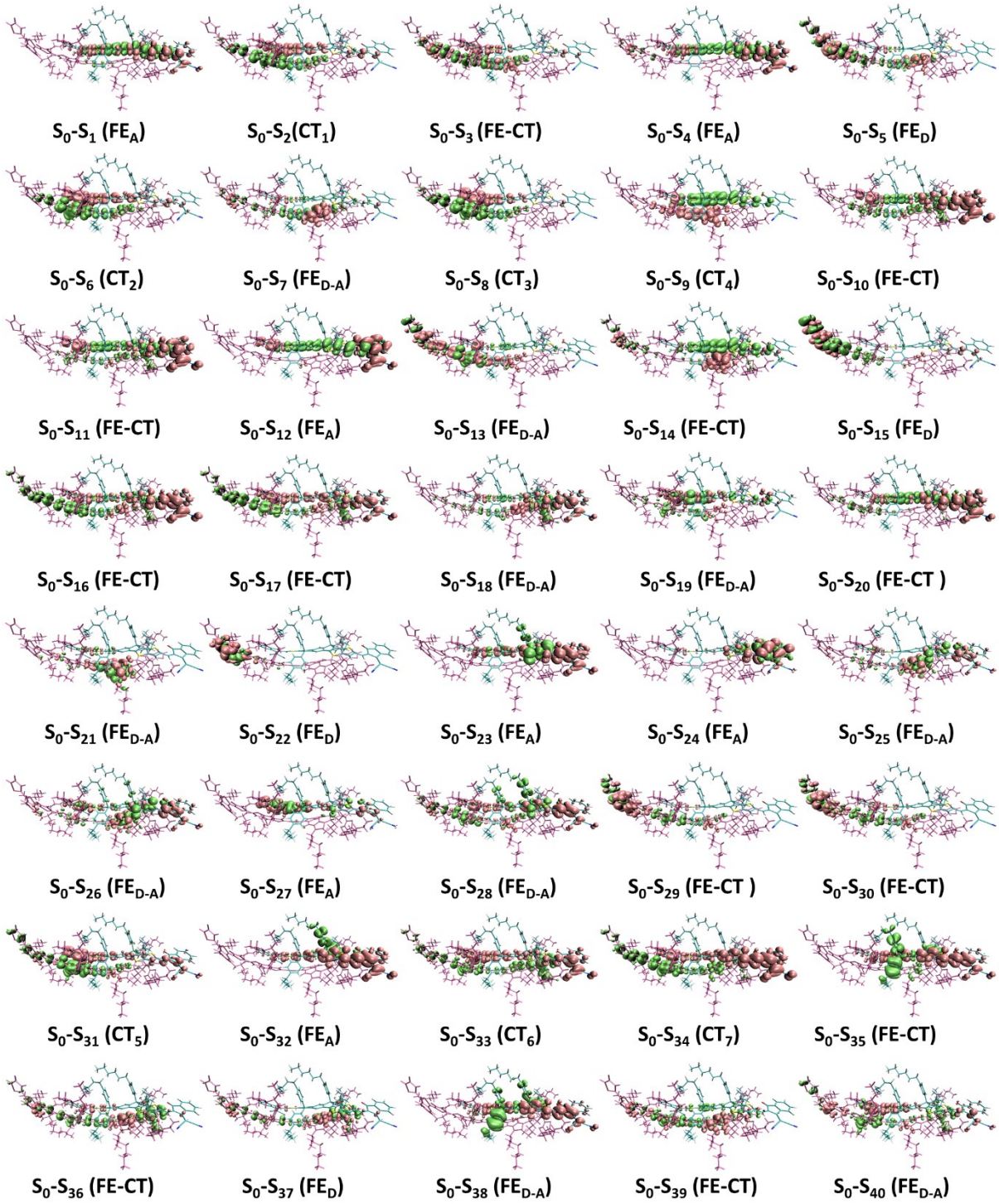

Fig. S2 Charge density difference (CDD) maps of the Frenkel excitons (FE) and charge transfer (CT) states among the lowest 40 excited states of the PBDB-TF/ITIC interface.

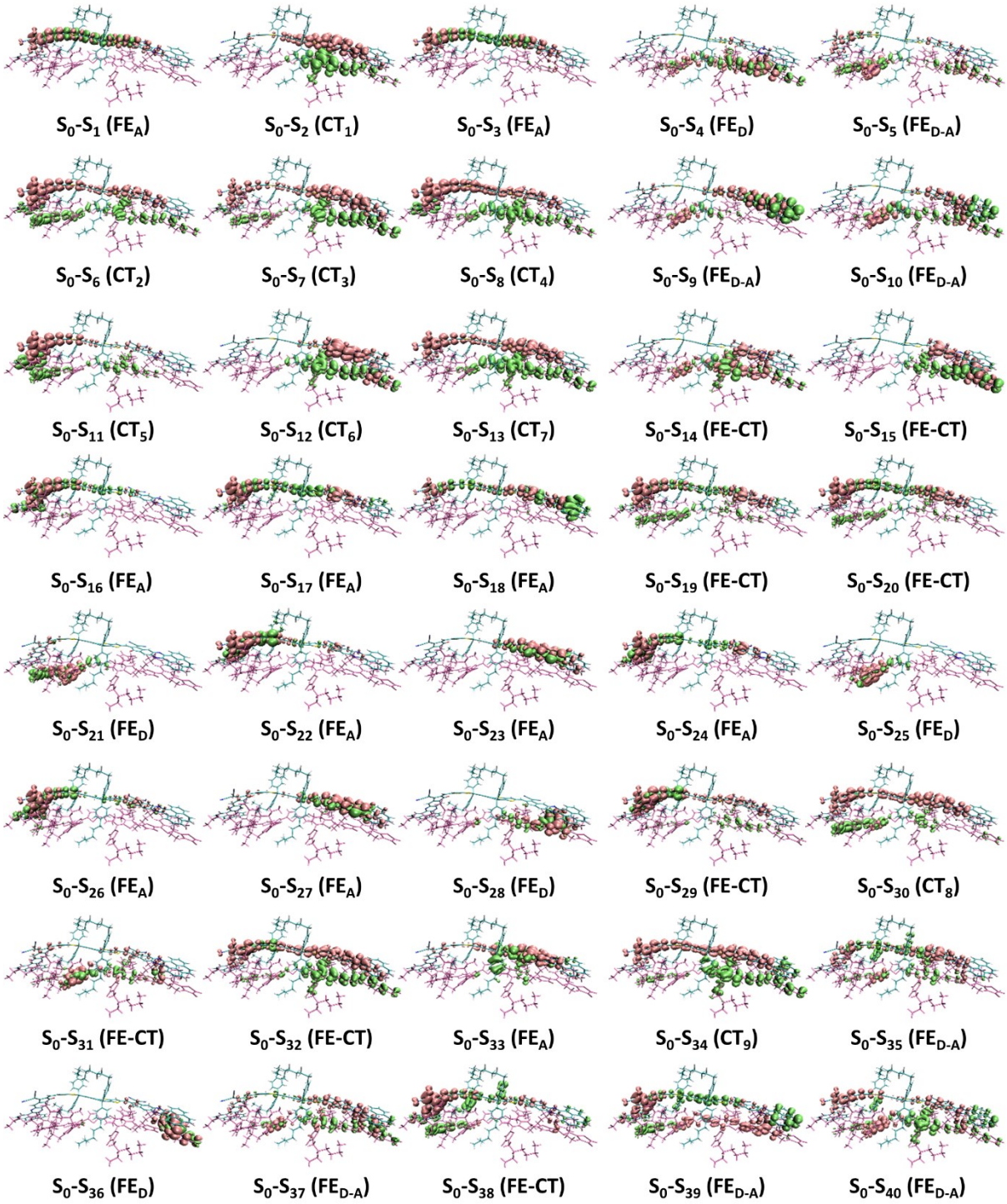

Fig. S3 Charge density difference (CDD) maps of the Frenkel excitons (FE) and charge transfer (CT) states among the lowest 40 excited states of the PBDB-TF/A5_h interface.

Table S1 Calculated energies related with the interfaces of PBDB-TF/ITIC and PBDB-TF/A5_h

Interface	$E_{D/A}$(a.u)	E_D(a.u)	E_A(a.u)	E_{BSSE}(a.u)	E_b(eV)
PBDB-TF/ITIC	-17941.015	-12347.056	-5593.820	0.046	-2.52
PBDB-TF/A5_h	-19386.894	-12347.041	-7039.657	0.058	-3.75

Table S2 Excitation energies (*E* and *λ*), oscillator strengths (*f*), and the amount of charge (Δ*q*) transferring from the donor to the acceptor for the lowest 40 excited states of the studied two interfaces

	PBDB-TF/ITIC				PBDB-TF/A5_h			
Excited state	*E*/eV	*λ*/nm	*f*	*Δq*/|e⁻|	*E*/eV	*λ*/nm	*f*	*Δq*/|e⁻|
S1	2.178	569.15	1.810	0.022	2.140	579.34	2.585	0.001
S2	2.399	516.78	0.983	0.740	2.285	542.65	0.022	0.974
S3	2.493	497.26	1.816	0.243	2.533	489.56	0.067	0.017
S4	2.646	468.67	0.138	0.002	2.637	470.11	2.049	0.029
S5	2.775	446.76	0.105	0.012	2.787	444.89	0.302	0.087
S6	2.880	430.51	0.002	0.906	2.820	439.69	0.174	0.799
S7	2.972	417.20	0.108	0.024	2.838	436.81	0.057	0.812
S8	3.085	401.88	0.030	0.921	2.999	413.37	0.089	0.738
S9	3.174	390.60	0.012	-0.802	3.034	408.59	0.343	0.037
S10	3.219	385.15	0.014	0.519	3.072	403.61	0.011	0.063
S11	3.243	382.32	0.014	0.361	3.095	400.61	0.121	0.494
S12	3.309	374.72	0.030	0.002	3.185	389.31	0.155	0.636
S13	3.332	372.12	0.153	0.004	3.201	387.30	0.013	0.923
S14	3.377	367.14	0.060	-0.610	3.263	379.98	0.438	0.142
S15	3.388	365.91	0.242	0.043	3.291	376.70	0.121	0.179
S16	3.400	364.63	0.044	0.609	3.306	374.99	0.014	0.051
S17	3.431	361.40	0.035	0.656	3.351	369.96	0.019	0.019
S18	3.454	358.93	0.298	0.199	3.362	368.83	0.091	0.073
S19	3.474	356.86	0.011	0.118	3.402	364.46	0.060	0.403
S20	3.492	355.07	0.007	0.182	3.424	362.12	0.022	0.336
S21	3.510	353.26	0.105	0.023	3.443	360.13	0.207	0.025
S22	3.546	349.65	0.027	0.000	3.444	360.00	0.012	0.039
S23	3.560	348.26	0.038	-0.001	3.465	357.82	0.006	-0.006
S24	3.587	345.65	0.005	-0.004	3.473	356.96	0.023	-0.003
S25	3.610	343.41	0.035	0.038	3.479	356.38	0.034	-0.005
S26	3.620	342.48	0.006	0.058	3.495	354.78	0.028	0.083
S27	3.628	341.71	0.013	0.006	3.511	353.18	0.011	0.052
S28	3.646	340.05	0.088	0.132	3.531	351.12	0.086	0.021
S29	3.664	338.34	0.023	0.055	3.557	348.60	0.004	0.188
S30	3.676	337.29	0.058	0.104	3.562	348.12	0.030	0.782
S31	3.704	334.72	0.019	0.628	3.564	347.86	0.059	0.154
S32	3.719	333.37	0.008	0.029	3.566	347.68	0.018	0.659
S33	3.752	330.46	0.017	0.810	3.579	346.41	0.080	0.125
S34	3.793	326.84	0.008	0.919	3.604	344.05	0.010	0.685
S35	3.825	324.15	0.009	0.076	3.619	342.62	0.028	0.164
S36	3.836	323.19	0.146	0.109	3.646	340.10	0.007	0.008
S37	3.874	320.02	0.022	0.032	3.650	339.65	0.088	0.131
S38	3.918	316.45	0.027	0.019	3.674	337.48	0.070	0.230
S39	3.930	315.46	0.278	-0.096	3.680	336.95	0.048	-0.147
S40	3.951	313.81	0.056	0.405	3.700	335.08	0.059	0.174